

Bi-axial behavior of glass/epoxy pipe subjected to internal pressure

Abdul Mateen Mohammed^{1,a*}, Tajuddin Mohammed^{2,b}, Ravi Shankar D V^{3,c}
Manzoor Hussain M^{4,d} and Puneetha^{5,e}

¹Associate Professor, School of Engineering and Technology, CMR University, Bengaluru - 562149, INDIA

²Department of Non-Destructive Engg & Tech (NDET), University of Hafr Al Batin, Hafr Al Batin, 39524, Kingdom of Saudi Arabia

³Department of Mechanical Engineering, TKR College of Engineering and Technology, Hyderabad, Telangana - 500 097, INDIA

⁴Department of Mechanical Engineering, Jawaharlal Nehru Technological University Hyderabad, Hyderabad, Telangana - 500 085, INDIA

⁵ Department of Mathematics, School of Engineering and Technology, CMR University, Bengaluru, Karnataka, 562149, INDIA

^{a*}abdulmateen7@gmail.com, ^btajmohammed@uhb.edu.sa, ^cshankardasari64@gmail.com,
^dmanzoorjntu@gmail.com, ^epuneethmath@gmail.com

Keywords: Open End Burst Test, GFRP, Bi-Axial Behaviour, Stress and Strain

Abstract. Composite structures are considered as the auxiliary to the conventional metallic materials. However, a thorough understanding of the material behaviour is required to replace the materials in use with scientific evidence for design rather than the designing based on high safety factor. The behaviour of filament wound E-glass/epoxy pipes of different helix angles exposed to internal pressure are studied. The sample GFRP pipe of different helix angles namely [$\pm 45^\circ$], [$\pm 55^\circ$] & [$\pm 70^\circ$] were subjected to open end pressure until the sample failed due to burst (pressure) and the corresponding strains were recorded using the strain smart 5000 data acquisition system (DAQ). The theoretical first-ply failure and burst pressure were determined using (i) Maximum stress theory, (ii) Maximum strain theory and (iii) Tsai Hill theory and were later compared with the experimental results. The first ply failure of the samples was observed by the whitening phenomenon. Later, the damage initiated by the formation of pine holes that act as a micro crack and which later grows to a macro crack in the fiber direction until final failure. A nonlinear relation between the longitudinal stress and strain was observed.

1. Introduction

Fiber reinforced polymeric (FRP) composites are considered analogues to the conventional materials such as metals for a specific advantage as these materials possess high strength to weight ratio. Among the few automated processing techniques used in the production of FRP components, filament winding method is the forthwith methodology that is available for production units where in a continuous fiber is carefully arranged in controlled direction. Predominantly, the filament-wound structures are axisymmetric shells, where the fibers are wound with $\pm\theta$ helix angle with respect to the symmetric axis. The properties like High strength to low weight ratio, provision for tailoring the material properties and corrosion resistance, has led to the use of these fiber reinforced structural components in many engineering applications. In general, these structures are subject to complex loading conditions and the mechanical performance of these structures depends on the helix angle used to develop the structures. The Contemporary advancements in the computer-control system and the design software has facilitated the designer to generate multiple winding sequences depending on specific requirement. Generally, to improve the productivity intermediate

angles between 0° and 90° are selected. However, the design procedure in specifying the lay-up depends on (a) the selection of fiber and matrix, (b) fiber layup in each layer, (c) the thickness of each lamina and (d) overall laminate thickness. While FRP pipes are tested under different mechanical loadings and pressures, the designer should note that the mechanical properties measured are affected by the internal pressure applied [1]. In general, the stress and failure analysis are normally carried out deprived of considering (i) the internal liner and (ii) the outer cover. It is assumed that these two parts, the inner liner and the outer cover would not contribute in resistance to deformation [2]. Composite pipes under internal pressure are exposed to both hoop and axial stresses with hoop-to-axial stress of 2:1. In the case of open ends tubes the axial stress produced in the structure due to the applied pressure is zero. Furthermore, auxiliary stresses may upshot due to installation, weight, external pressure, etc.

A preliminary structure to regulate the failure of GRE pipes in its function, which was imperiled to hydrostatic internal pressure was considered by Roham and Farshid [3] in order to inquire about the factures such as (i) winding angle and (ii) fibre volume fraction on the failure. Five distinct fiber volume fractions ranging from 50%-60% with an increment of 2.5% along with three specific winding angles, (i) $\pm 52.5^\circ$, (ii) $\pm 57.5^\circ$, and (iii) $\pm 60.9^\circ$ were considered to resolve the first ply failure (FPF) and burst pressures. Failure test of a composite tube at normal ambient temperature and at the higher temperature of 100°C was conducted by P. Mertiny et al [4]. This failure test basically a leakage was done by means of a permeability-based and fluid volume loss methodology. In the course of the analysis, the leakage in the tube was found based on two phenomenon, (i) the aggregate loss in the volume of the fluid and (ii) the active permeability established with reference to the average fluid flux. A composite tubes with the $\pm 60^\circ$ winding angle was pressurization by a hydraulic oil in a closed ended condition. The pressure was perpetually augmented under three steps of the loading, and later it was reported that the leakage stress had a direct relation with the loading rate.

Rosenow [5] tested the pipes made of GRP individually under different loading cases (i) biaxial pressure (ii) tensile and (iii) hoop pressure. The samples with a diameter of 50.8 mm were made of six different winding angles ranging between 15° - 85° with an increment of 15 degrees. The axial and hoop strains were measured using strain gauges which were later contrasted with the strain values calculated based on classical lamination theory (CLT) and a good similitude was reported. The optimum winding angle for the pipe under the biaxial pressure loading was 54.75° and 75° for hoop pressure loading was concluded. It was quantified that CLT could be reliable until the nonlinearity point is obtained.

Spencer and Hull [6] has considered GRP with four winding patterns namely $\pm 35^\circ$, $\pm 45^\circ$, $\pm 65^\circ$ and $\pm 75^\circ$ with an internal diameter of 50 mm for the study under internal pressure. And the study strongly demonstrated that the failure mechanism and the deformation are intensely influenced by the winding angles. The failure structure from weepage to the burst was along with the deformation characteristic were decided using strain gauges which were mounted along the hoop and axial directions of pipes.

Arikan [7.] evaluated the failure behaviour of filament wound pipes which possess an inclined crack along the surface under internal pressure. The helix angle was maintained at $[\pm 55^\circ]$ for all the specimens as the orientation of surface crack angles was varied from 0° to 90° , with an increment of 15° along the longitudinal axis of the specimen. The failure was under three stages, however, the pattern of failure that occurred is not reported. Hugo [8] implemented the European standards, EN1447 and EN1227 to investigate the extended properties on a scale down test pool of GFRP pipe. The Ultimate Elastic Wall Stress (UEWS) along with the strain to failure tests, ascertains the first non-elastic behaviour, which furnishes a surrogate explanation to anticipate the abiding hydrostatic pressure strength [9, 10]. Under the biaxial and hydrostatic loading conditions filament wound glass fiber reinforced epoxy (GRE) composite pipes at varying temperatures up to

95 °C were subjected to test by Majid et al [11.–15.]. Wherein they have used a UEWS test that is a momentary test operated by the manufacturing companies in-order to assure the combat protracted functioning of pipes under regression test as per the ISO 14692 through ASTM D2992. However, the failure behaviour and the failure pattern of these materials are further needed to be understood so that the designers could effectively utilizes these materials for further more applications. Thus, the present paper aims at determining the internal burst pressure capacity of glass/epoxy pipes for different winding angles required for pressure vessel applications. The theoretical first-ply failure & burst pressure based on Tsai Hill theory, Maximum strain theory and Maximum stress theory were used as baseline and compared with experimental results. The filament wound GFRP pipes of different helix angles namely $[\pm 45^\circ]$, $[\pm 55^\circ]$ & $[\pm 70^\circ]$ are pressurized until they burst with water as medium using hand operated pump and strains were recorded using the DAQ.

2. Experimentation:

The experiments were conducted using a open-end burst test on the samples made from E-glass/epoxy and the procedure of sample preparation and the testing is detailed in the sub section below.

2.1. Sample preparation

The E-glass/epoxy pipe samples required for the present study were produced using the filament winding facility available at CNC Techniques, Hyderabad, India. The pipes were of two-meter length, 50mm internal diameter and 3mm thickness, with three different fiber orientations, $[\pm 45^\circ]$, $[\pm 55^\circ]$ and $[\pm 70^\circ]$. The pipes after winding on the mandrel were allowed to cure under an IR heater, which was maintained at a temperature of 1300C while the mandrel was rotating at very low speed. After the samples were cured, a 600 mm length tubes were cut using a diamond dust cutter and the ends were prepared for the open-end burst test. A small piece from each sample was take in-order to determine the volume fraction using burn test and was found to be 58%. At the Centre of the pipe sample, a rosette type strain gauge was bonded and care was taken during bonding so as to form a perfect bond between the sample and the strain gauge.

2.2. Test Equipment

The experiments were conducted on the test set-up similar to that of the open- end burst test by P. D. Soden, et al. [13], however instead of the hydraulic power pack a hand operated pump was used to pressurize the system with trivial modifications. Figure 1 describes the test set-up used in the nonce study for testing GFRP pipes under internal pressure. The test set-up comprises of (i) Mechanical Structure and (ii) Strain measuring unit. The mechanical structure constitutes of a hand operated pump used to pressurize the system that is connected to a non-return valve. The other side of the non-return valve is connected to one of the two end caps that are used to firmly hold the sample. The end caps are provided with a circular groove in them, so as to accommodate the pipe and rubber seal. The sample is fixed using four tie rods which are of sufficient strength to restrict the leakage at the plates. The strain measuring system consists of strain smart 5000 data acquisition system (DAQ) from Micro Measurements which has an in-built compensation circuit required for completing the bridge circuit, depending on the resistance of the strain gauge.

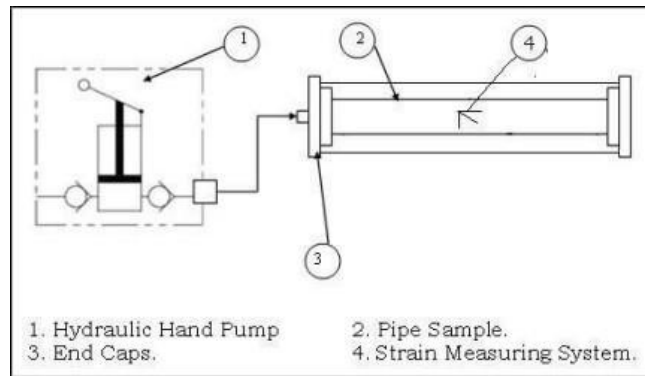


Fig 1: Schematic diagram for pipe burst test.

3. Results and Discussion

The pipe samples with orientation mentioned earlier were subjected to burst test using the test equipment described above. The system was pressurized until the sample fail due to burst and the equivalent strains were logged using the DAQ system. The theoretical first-ply failure and burst pressure were anticipated using (i) Tsai Hill theory, (ii) Maximum strain theory and (iii) Maximum stress theory which were later compared with the experimental results. The results obtained from the experimentation and the theoretical prediction of first-ply failure and the burst failure are tabulated in table 1. The experimental burst pressures for the sample with $[\pm 45^\circ]$, $[\pm 55^\circ]$ and $[\pm 70^\circ]$ fiber orientation is found to be 4.383 MPa, 7.71 MPa and 4.2762 MPa respectively. However, in the present study the first ply failure of the samples was observed in the form of whitening phenomenon which occurred on the sample during the test.

The stress – strain relation for the sample with $[\pm 45^\circ]$, $[\pm 55^\circ]$ and $[\pm 70^\circ]$ fiber orientation is represented in fig 2-4. A nonlinear stress – strain behaviour was witnessed intended for the samples in the longitudinal direction, however for the sample with $[\pm 70^\circ]$ fiber orientation the stress – strain relation was in the positive side indicating a tensile stress state induced in the sample. A linear stress strain relation is observed till the theoretical first ply failure for the sample with $[\pm 45^\circ]$ and $[\pm 55^\circ]$ fiber orientations which later changes to nonlinear until the final failure. Moreover, the nonlinear behaviour for the sample with $[\pm 45^\circ]$ fiber orientation due to the sliding of the fiber the strain changes its sign.

Table 1. Comparison between the experimental results and the failure theories.

Winding Angle	First Ply Failure		Burst Pressure				
	Maximum Stress theory	Maximum Strain theory	Tsai Hill theory	Experimental	Maximum Stress theory	Maximum Strain theory	Tsai Hill theory
Deg	in MPa						
$[\pm 45^\circ]$	2.84402	2.36137	2.42798	4.38311	4.66024	4.66024	3.58222
$[\pm 55^\circ]$	5.4781	3.31578	3.97099	7.70968	7.25047	6.26064	6.87799
$[\pm 70^\circ]$	2.63801	2.11788	2.41895	4.27618	4.46159	4.17592	4.27333

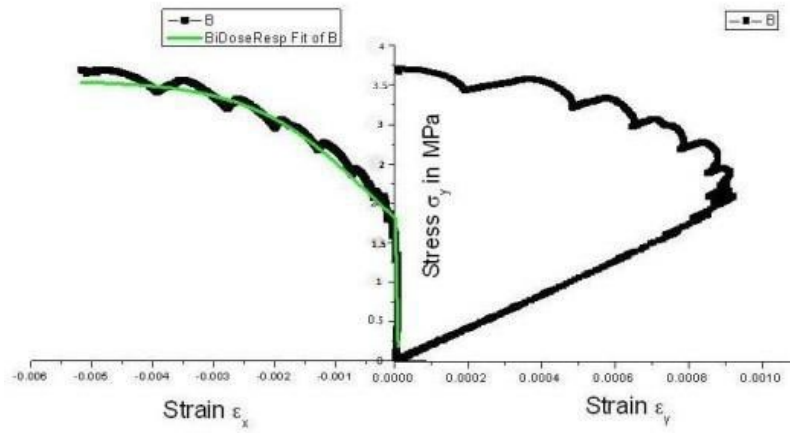


Fig 2: Stress – Strain distribution for $[\pm 45^\circ]$ sample under $S.R=1:0$.

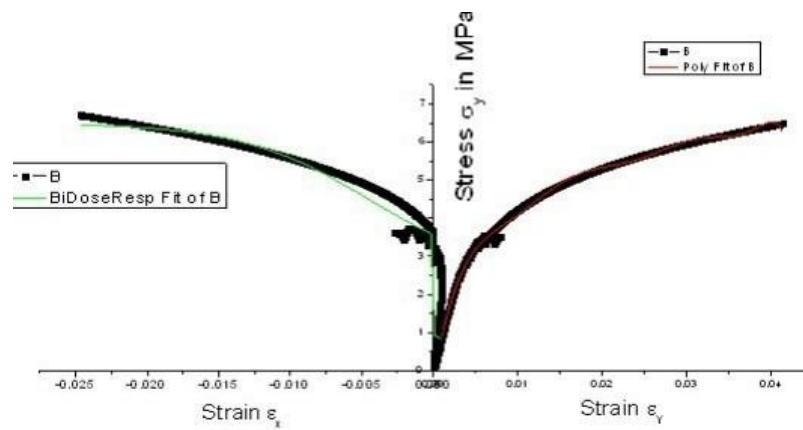


Fig 3: Stress – Strain distribution for $[\pm 55^\circ]$ sample under $S.R=1:0$.

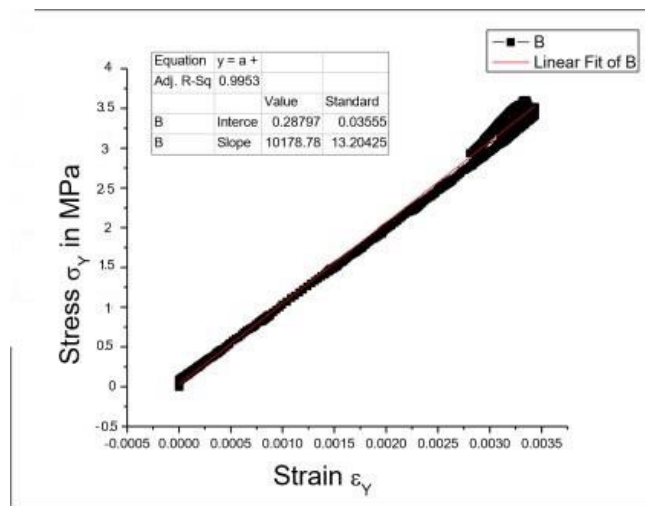


Fig 4: Longitudinal Strain distribution for $[\pm 70^\circ]$ sample under $S.R=1:0$.

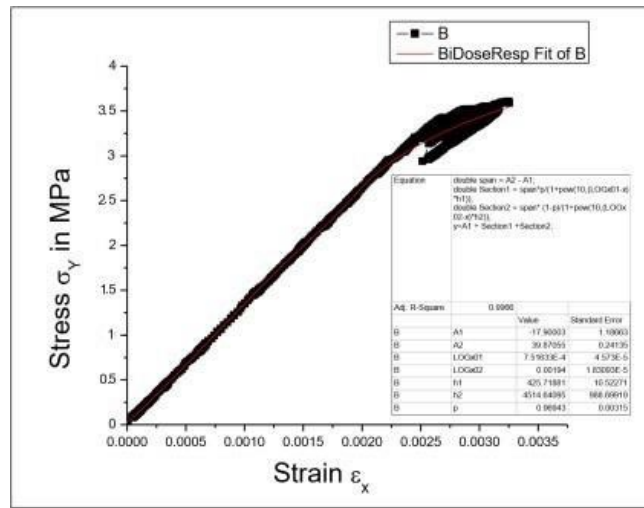


Fig 5: Hoop Strain Distribution for $[\pm 70^\circ]$ sample under $S.R=1:0$.

The failure pattern which is represented in the fig 6 indicates an outflow along the pipe body. The close view at the middle of the pipe sample indicates the appearance of crack between fiber and matrix when attitude to the pressure being applied. Furthermore, there are numerous cracks along the axial direction at final failure position indicated in Figure 6(c), representing a larger stress along the circumferential direction is being experienced by the outer wall of the sample which is a resin-rich layer. These axial cracks are the typical mode of failure that the GFRP pipe experiences due to the internal pressure. Two different types of failure patterns were typically found when the crack morphology at the failure was observed with naked eye. The first one being the appearance of fiberglass whitening along the area of failure and the second being a great number of cracks along the circumferential direction. Besides the presence of the cracks along the circumferential direction there are small pin holes which are also the axial cracks which can be seen in Fig 6(a). These pin holes are found in large number on the sample which are caused owing to the fiber fracture. Though these pin holes could be viewed as the part of the circumferential cracks that are appeared along the sample which are the damage initiation sites. These damage initiation i.e., the pine holes which form a micro crack, later grows into a macro crack to form a thin white line parallel to the fiber direction, which is highlighted in fig 6(a&c). This whitening, originates to a matrix crack followed by fiber–matrix de-bonding which are produced due to the shearing of matrix which occurs parallel to the fiber. The whitening physical process has been even reported by other investigators and was ascribe mainly due to the matrix cracking and local interface debonding. A careful examination indicated that the damage or microcracked in a band form proliferates about the fibres without effecting the interface between the fibre and matrix which is represented in fig 7.

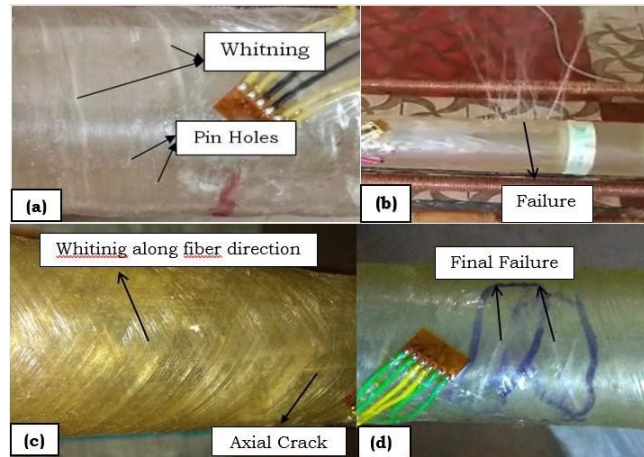


Fig 6: Macroscopic Failure Morphology of the failed sample.



Fig 7: Morphology of failure along the fiber direction.

Conclusions

GFRP Tubular samples with three different fiber lay-up configurations, i.e. $[\pm 45^\circ]$, $[\pm 55^\circ]$ and $[\pm 70^\circ]$, were tested under internal pressure with open end burst test arrangement. Data in the form of strains with respect to the applied stress were recorded using a strain smart data acquisition system. Later the stresses at both the functional and structural breakdown, along with the stress-strain relation were computed and following conclusions are drawn:

1. The experimental results signify that the samples with different winding angles failed at different burst pressures. The sample with $[\pm 45^\circ]$ fiber orientation failed under burst at 4.38311 MPa whereas the sample with $[\pm 55^\circ]$ and $[\pm 70^\circ]$ fiber orientation failed at 7.70968 MPa, 4.27618 MPa respectively.

2. The sample with $[\pm 45^\circ]$ and $[\pm 55^\circ]$ fiber orientation showed a nonlinear stress – strain behaviour. However, the sample with $[\pm 70^\circ]$ indicated an approximate linear relation between the applied stress and the longitudinal strain.

3. The samples with $[\pm 45^\circ]$ and $[\pm 55^\circ]$ fiber orientation indicated a linear stress strain relation until the theoretical first ply failure (both in longitudinal and hoops direction); later the behaviour changes to non-linear. Moreover, the strain in the hoops direction decreases after the first ply failure for the $[\pm 45^\circ]$ sample indicating a strain reliving phenomena.

4. A micro crack is observed as pin holes on the sample just before the first fly failure which later increases in number with an increase in pressure. These pin holes become unstable and propagates along the fiber direction after the theoretical first ply failure. Theses micro cracks

accumulate and grow in to macro cracks along the fiber direction and appear as white lines along the fiber direction.

Acknowledgments

The authors would like to acknowledge the support rendered by CNC Technology, Hyderabad in preparation of samples. The authors would like to thank Mr. K. Vidya Sagar, Founder Vijaya Duraga Associates, Hyderabad for providing the strain smart data acquisition system during the test schedule.

Reference

- [1] P. A. Zinoviev, S. V. Tsvetkov, Mechanical properties of unidirectional organic-fiber reinforced plastics under hydrostatic pressure, *Composites Science and Technology* 58 (1998) 31-9. [https://doi.org/10.1016/S0266-3538\(97\)00079-1](https://doi.org/10.1016/S0266-3538(97)00079-1)
- [2] DNVGL-RP-F119, Recommended Practice for Thermoplastic composite pipes, Technical Report, DNV GL, 2015.
- [3] R. Rafiee, F. Reshadi, Simulation of functional failure in GRP mortar pipes, *Compos. Struct.* 113 (2014) 155-163. <https://doi.org/10.1016/j.compstruct.2014.03.024>
- [4] P. Mertiny, A. Gold, Quantification of leakage damage in high-pressure fibre reinforced polymer composite tubular vessels, *Polym. Test.* 26 (2) (2007) 172-179. <https://doi.org/10.1016/j.polymertesting.2006.09.009>
- [5] Rosenow MWK. Winding angle effects in glass fibre reinforced polyester filament wound pipes. *Composites* 1984;15(2):144-52. [https://doi.org/10.1016/0010-4361\(84\)90727-4](https://doi.org/10.1016/0010-4361(84)90727-4)
- [6] Spencer B, Hull D. Effect of winding angle on the failure of filament wound pipes. *Composites* 1978;263- 71. [https://doi.org/10.1016/0010-4361\(78\)90180-5](https://doi.org/10.1016/0010-4361(78)90180-5)
- [7] Arikan H. Failure analysis of ($\pm 55^\circ$) filament wound composite pipes with an inclined surface crack under static internal pressure. *Compo Struct* 2010;92 (1):182-7. <https://doi.org/10.1016/j.compstruct.2009.07.027>
- [8] H.F. Schwencke, The use of the ultimate elastic wall stress (UEWS) in evaluating PVC polymer blends, *J. Vinyl Technol.* 11 (1) (1989) 28-32. <https://doi.org/10.1002/vnl.730110108>
- [9] H. Faria, R.M. Guedes, Long-term behaviour of GFRP pipes: reducing the prediction test duration, *Polym. Test.* 29 (3) (2010) 337-345. <https://doi.org/10.1016/j.polymertesting.2009.12.008>
- [10] T.A. Assaleh, L.A. Almaguz, Ultimate elastic wall stress (UEWS) test under biaxial loading for glass-fibre reinforced epoxy (GRE) pipes, *Adv. Mater. Res.* 974 (2014) 188-194. <https://doi.org/10.4028/www.scientific.net/AMR.974.188>
- [11] M.S. Abdul Majid, M. Afendi, R. Daud, N.A.M. Amin, A. Mohamad, E.M. Cheng, M. Hekman, General lifetime damage model for glass fibre reinforced epoxy (GRE) composite pipes under multiaxial loading, *Key Eng. Mater.* 594 (2014) 624-628. <https://doi.org/10.4028/www.scientific.net/KEM.594-595.624>
- [12] M.S. Abdul Majid, A.G. Gibson, M. Hekman, M. Afendi, N.A.M. Amin, Strain response and damage modelling of glass/epoxy pipes under various stress ratios. *Plastics, (2014) 290-Rubber and Composites*, 299. <https://doi.org/10.1179/1743289814Y.0000000101>
- [13] M.S. Abdul Majid, M. Afendi, R. Daud, A.G. Gibson, T.A. Assaleh, J.M. Hale, M. Hekman, Acoustic emission monitoring of multiaxial ultimate elastic wall stress tests of glass

fibre-reinforced epoxy composite pipes, *Adv. Compos. Mater.* (2014) 1-17.
<https://doi.org/10.1080/09243046.2013.871175>

[14] M.S. Abdul Majid, M. Afendi, R. Daud, A.G. Gibson, M. Hekman, Effects of winding angles in biaxial ultimate elastic wall stress (UEWS) tests of glass fibre reinforced epoxy (GRE) composite pipes, *Adv. Mater. Res.* 795 (2013) 424-428.
<https://doi.org/10.4028/www.scientific.net/AMR.795.424>

[15] M.S. Abdul Majid, T.A. Assaleh, A.G. Gibson, J.M. Hale, A. Fahrer, C.A.P. Rookus, M. Hekman, Ultimate elastic wall stress (UEWS) test of glass fibre reinforced epoxy (GRE) pipe, *Compos. A: Appl. Sci. Manuf.* 42 (10) (2011) 1500-1508.
<https://doi.org/10.1016/j.compositesa.2011.07.001>

[16] Qi Guoquan¹, Qi Dongtao¹, Bai Qiang¹, Li Houbu¹, Wei Bin¹, Ding Nan¹, Zhang Dongna¹, and Shao Xiaodong, Failure Analysis on Pressure Leakage of FRP, *Fibers and Polymers* 2019, Vol.20, No.3, 595-60. <https://doi.org/10.1007/s12221-019-8617-5>